Intersystem Crossing Dynamics in the Iron(III) Spin-Crossover Compounds $[Fe(acpa)_2]PF_6$ and $[Fe(Sal_2tr)]PF_6$

Sabine Schenker,[†] Andreas Hauser,*[,†] and Raylene M. Dyson[‡]

Institut für anorganische und physikalische Chemie, Universität Bern, Freiestrasse 3, CH-3012 Bern, Switzerland, and Department of Chemistry, University of Newcastle, Callaghan, NSW 2308, Australia

Received January 5, 1996[⊗]

The high-spin → low-spin relaxation dynamics of the Fe(III) spin-crossover complexes $[Fe(Sal_2tr)]PF_6$ (H_2Sal_2tr = Bis(salicylaldimino)triethylenetetramine) and $[Fe(acpa)_2]PF_6$ (Hacpa = *N*-(1-acetyl-2-propylidene)-2-pyridylmethylamine) are discussed within the theory of nonadiabatic multiphonon relaxation. A Huang−Rhys factor *S* of ≈25, estimated on the basis of average metal−ligand bond length differences Δr_{HL} of ≈ 0.12 Å, explains the observed low-temperature tunneling rate constants $k_{HL}(T\rightarrow 0)$ of ≈ 10^2 s^{-1} as well as the thermally activated process at $T >$ ≈100 K semiquantitatively. The results obtained for the Fe(III) compounds are compared to those for Fe(II) spin-crossover compounds.

1. Introduction

Intersystem crossing (ISC) processes are crucial in a large number of technologically important photophysical and photochemical applications of coordination compounds. Understanding the parameters which govern their rate constants and quantum efficiencies not only qualitatively but quantitatively is thus of more than just academic interest. Spin-crossover compounds of first-row transition metal ions, that is, compounds of d^4−d^7 ions showing an entropy driven transition from a low-spin (LS) state at low temperatures to a high-spin (HS) state at elevated temperatures,[1] are model systems for studying ISC dynamics. There are a number of experimental methods available such as Raman laser temperature jump,[2,3] ultrasonic relaxation,[2,4] and pulsed laser excitation,[2,5] and there are no competing processes interfering with the process in question. Furthermore, it is possible to determine the relevant structural and energetic parameters independently, as for instance the difference in metal−ligand bond length Δr_{HL} and the zero-point energy difference ΔE°_{HL} between the HS and the LS state.

Some 15 years ago Buhks et al.[6] suggested that ISC dynamics in spin-crossover compounds should be treated as a nonadiabatic process within the theory of radiationless multiphonon relaxation. They predicted the HS → LS relaxation to be a thermally activated process at elevated temperatures with a nonvanishing tunneling rate at cryogenic temperatures. For the HS ($^5T_2$) → LS ($^1A_1$) relaxation in Fe(II) compounds this prediction was subsequently shown to be true.[7,8] In particular, the exponential increase of the low-temperature tunneling rate constant $k_{HL}(T\rightarrow 0)$ with increasing zero-point energy difference ΔE°_{HL} (inverse energy gap law) expected in the limit of strong vibronic coupling, that is, in the limit of small vertical (ΔE°_{HL}) and large horizontal shift (Δr_{HL}) of the potential wells of HS and LS state relative to each other, could be verified experimentally.[8,9] Furthermore, the extremely long-lived light-induced HS states,[8−11] with low-temperature lifetimes of 10^2−10^6 s could be explained semiquantitatively based on the value of Δr_{HL} for Fe(II) compounds of ≈0.16−0.21 Å.[12−16]

Despite the fact that at ambient temperatures HS → LS relaxation rate constants for Fe(III) spin-crossover compounds are typically only 1 order of magnitude larger than for Fe(II) systems, that is $10^{8\pm1}$ s^{-1} versus $10^{7\pm1}$ s^{-1},[3−5,15,16] no reports of long-lived metastable states at low temperatures for the former have appeared in the literature so far.

The title compounds $[Fe(Sal_2tr)]PF_6$ (H_2Sal_2tr = Bis(salicylaldimino)triethylenetetramine),[3] $[Fe(acpa)_2]PF_6$ (Hacpa = *N*-(1-acetyl-2-propylidene)-2-pyridylmethylamine),[17] and the related $[Fe(bzpa)_2]PF_6$ (Hbzpa = *N*-(1-benzoyl-2-propylidene)-2-pyridylmethylamine)[18] are reported to be spin-crossover systems in the solid state. In $[Fe(Sal_2tr)]PF_6$ the spin-transition occurs at a temperature $T_{1/2}$ (defined as the temperature for which the equilibrium constant is unity) of ≈200 K for one of the two crystallographically nonequivalent $[Fe(Sal_2tr)]^+$ species, whereas the other species seems to have a $T_{1/2}$ below 100 K.[19] [Fe(acpa)$_2$]PF_6 and $[Fe(bzpa)_2]PF_6$ have transition temperatures of

[†] Universität Bern.
[‡] University of Newcastle.
[⊗] Abstract published in *Advance ACS Abstracts,* July 15, 1996.

(1) Gütlich, P. In *Advances in Mössbauer Spectroscopy*; Herber, R. H., Ed.; Plenum Press: New York, 1984; p 27.
(2) Beattie, J. K. *Adv. Inorg. Chem.* **1988**, *32*, 1.
(3) Tweedle, M. F.; Wilson, L. J. *J. Am. Chem. Soc.* **1976**, *98*, 4824.
(4) Binstead, R. A.; Beattie, J. K.; Dose, E. V.; Tweedle, M. F. ; Wilson, L. *J. Am. Chem. Soc.* **1978**, *100*, 5609.
(5) Lawthers, I.; McGarvey, J. *J. Am. Chem. Soc.* **1984**, *106*, 4280.
(6) Buhks, E.; Navon, G.; Bixon, M.; Jortner, J. J. *Am. Chem. Soc.* **1984**, *106*, 2918.
(7) Xie, C. L.; Hendrickson, D. N. *J. Am. Chem. Soc.* **1987**, *109*, 6981.
(8) (a) Hauser, A.; Vef, A.; Adler, P. *J. Chem. Phys.* **1991**, *95*, 8710. (b) Vef, A.; Manthe, U.; Gütlich, P.; Hauser, A. *J. Chem. Phys.* **1994**, *101*, 9326.
(9) Hauser, A. *Comments Inorg. Chem.* **1995**, *17*, 17.
(10) Decurtins, S.; Gütlich, P.; Köhler, C. P.; Spiering, H.; Hauser, A. *Chem. Phys. Lett.* **1984**, *139*, 1.
(11) (a) Decurtins, S.; Gütlich, P.; Hasselbach, K. M., Spiering, H.; Hauser, A. *Inorg. Chem.* **1985**, *24*, 2174. (b) Decurtins, S.; Gütlich, P.; Hasselbach, K. M.; Spiering, H. *J. Chem. Soc., Chem. Commun.* **1985**, 430.
(12) Hoselton, M. A.; Wilson, L. J.; Drago, R. S. *J. Am. Chem. Soc.* **1975**, *97*, 1722.
(13) Mikami-Kido, M.; Saito, Y. *Acta Crystallogr.* **1982**, *B38*, 452.
(14) Wiehl, L.; Kiel, G.; Köhler, C. P.; Spiering, H; Gütlich, P. *Inorg. Chem.* **1986**, *25*, 1565.
(15) König, E. *Prog. Inorg. Chem.* **1987**, *35*, 527.
(16) König, E. *Struct. Bonding (Berlin)* **1991**, *76*, 53.
(17) Maeda, Y.; Tsutsumi, N.; Takashima, Y. *Inorg. Chem.* **1984**, *23*, 2440.
(18) Maeda, Y.; Tsutsumi, N.; Takashima, Y. *Chem. Phys. Lett.* **1982**, *88*, 248.
(19) Nishida, Y.; Oshio, H.; Takashima, Y.; Nikuriya, M. *J. Chem. Soc., Dalton Trans.* **1987**, 1957.

S0020-1669(96)00010-9 CCC: $12.00

$\approx$ 188 K[20,21] and 245 K,[18] respectively. The fact that for all threecompounds the thermal spin transition is of the gradual type indicates that cooperative effects are not dominant in these systems.

In a preliminary report,[22] we demonstrated that for the Fe(III) spin-crossover compound $[Fe(acpa)_2]PF_6$ the HS ($^6A_1$) $\rightarrow$ LS ($^2T_2$) relaxation following pulsed laser excitation shows the expected low-temperature tunneling process with a tunneling rate constant $k_{HL}(T\rightarrow 0)$ of $\approx 10^2$ s^{-1}, which is several orders of magnitude larger than that for Fe(II) spin-crossover compounds.

In this paper we present the results obtained on the above Fe(III) compound as well as the related $[Fe(bzpa)_2]PF_6$ and $[Fe(Sal_2tr)]PF_6$ in various matrices down to cryogenic temperatures. We discuss them in relation to solution data obtained at ambient temperatures[3-5] and in comparison to Fe(II) spin-crossover compounds.

2. Experimental Section

2.1. Preparation of Compounds. The compounds $[Fe(acpa)_2]PF_6$ and $[Fe(bzpa)_2]PF_6$ were prepared as described in the literature.[17,18] $[Fe(Sal_2tr)]PF_6$ was synthesized according to the literature[3] and characterized by elemental analysis. Anal. Calcd for $FeC_{20}H_{24}N_4O_2PF_6$: Fe, 10.09; C, 43.42; H, 4.37; N, 10.13; F, 20.60. Found: Fe, 10.50; C, 43.37; H, 4.24; N, 10.00; F, 20.40; H_2O, 0.54. $[In(Sal_2tr)]PF_6$ was prepared following the same procedure. X-ray powder diffraction showed that the two compounds are not isostructural. On the basis of IR spectra it was concluded that the pertinent $[In(Sal_2tr)]^+$ complex had formed. Diluted mixed crystals of $[In_{1-x}Fe_x(Sal_2tr)]PF_6$, $x = 0.005$ and 0.02, were grown by slow evaporation of a diethyl ether/acetone solution. The resulting crystals are dichroic. Under a polarization microscope they are reddish brown in one polarization and light orange perpendicular to it.

2.2. Physical Measurements. Physical measurements were performed on $[In_{1-x}Fe_x(Sal_2tr)]PF_6$ mixed crystals and on $[Fe(Sal_2tr)]PF_6$ dissolved in proprionitrile/butyronitrile (4:5) (P/Bn) and dispersed in KBr, as well as on $[Fe(acpa)_2]PF_6$ and $[Fe(bzpa)_2]PF_6$ dissolved and dispersed in the same matrices. The former is very suitable for low-temperature studies as it gives a good low-temperature glass ($T_g \approx$ 120 K).

Variable temperature absorption spectra in the visible were recorded with a Cary 5e spectrophotometer in conjunction with a closed-cycle refrigerator (Air Products) or a cold helium gas flow technique for temperatures between 10 K and room temperature.

As Fe(III) spin-crossover compounds generally do not luminesce, laser flash photolysis experiments were performed using the pump probe technique. For the excitation a pulsed dye laser (Lambda Physik FL3002; dyes = DCM, Pyridin 1, Rhodamin B) pumped by the second harmonic of a Q-switched ND/YAG laser (Spectra Physics DCR III) was used: repetition rate 20 Hz, pulse width 7 ns, and pulse energy < 1 mJ at the sample. The excitation beam was slightly off axis to the probe beam from a 100 W tungsten lamp, and the two were made to coincide at the sample. After having passed through the sample, the probe beam was dispersed in a $^1/_4$ m double monochromator (Spex 1680B) and detected with a PM tube (R928) in conjunction with a fast preamplifier (LeCroy VV100BTB). Excited state decay curves at fixed wavelength were recorded using a digital scope (Tektronix 2340 A). Excited state difference spectra were determined using a gated boxcar averager system (Stanford Research SR250). Sample temperatures down to 10 K were achieved using a cold helium flow technique or a closed cycle refrigerator system. Experiments at 100 K were performed in a bath cryostat (Oxford Instruments MD 4) using liquid N_2.

3. Results

3.1. Absorption Spectra. Figure 1a shows the temperature dependent absorption spectra of $[Fe(acpa)_2]PF_6$ in P/Bn ($\approx$5 mM, $d = 0.1$ cm) between 10 and 293 K (Due to an unfortunate data handling error, the spectra given in ref 22 differ somewhat from the spectra given here). The absorption band at 14 680 cm^{-1} ($\epsilon_{max}^{10\,K} = 1550$ L/mol cm), the intensity of which decreases with increasing temperature, can be assigned to the LS species. In contrast, the band at 17 600 cm^{-1} ($\epsilon_{max}^{295\,K} = 1640$ L/mol cm) showing the opposite temperature dependence is characteristic for the HS species. With extinction coefficients on the order of 10^3 L/mol cm both bands correspond to spin-allowed ligand-to-metal charge transfer (LMCT) transitions, that is $^2T_2 \rightarrow {}^2$LMCT for the LS species and $^6A_1 \rightarrow {}^6$LMCT for the HS species, respectively.

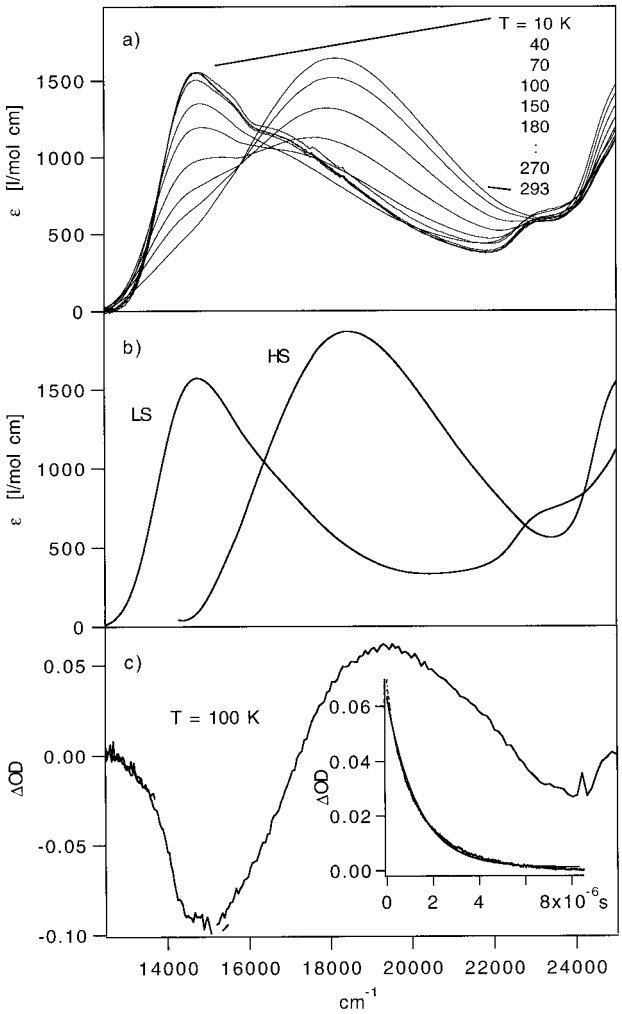

Figure 1. (a) Absorption spectra of $[Fe(acpa)_2]PF_6$ in P/Bn between 10 and 273 K. (b) Least-squares global fit to the experimental data with ΔH°_{HL} and ΔS°_{HL} as free parameters. (c) Excited state difference absorption spectrum of $[Fe(acpa)]_2$ PF_6 in P/Bn after pulsed laser excitation at 14 700 and 15 600 cm^{-1} at 100 K. Inset: HS $\rightarrow$ LS relaxation curve of $[Fe(acpa)_2]PF_6$ in P/Bn at 100 K detected at 18 380 cm^{-1} after pulsed laser excitation at 14 700 cm^{-1}.

In order to extract a thermal transition curve, that is the HS fraction γ_{HS} as a function of temperature for the LS $\rightleftharpoons$ HS equilibrium, a least-squares global fit[23] to the experimental spectra with ΔH°_{HL} and ΔS°_{HL} as free parameters was performed. Figure 1b shows the resulting most probable spectra of the pure LS and HS species, respectively. The LS spectrum is in good agreement with the experimental spectrum at 10 K, implying that at low temperatures $\gamma_{HS} \rightarrow 0$. The HS spectrum, however, is substantially different from the experimental spectrum at 295 K, indicating that at 295 K the LS fraction γ_{LS} is still $\approx$0.3.

(20) Maeda, Y.; Oshio, H.; Takashima, Y.; Mikuriya, M.; Hidaka, M. *Inorg. Chem.* **1986**, *25*, 2958.
(21) Sorai, M.; Maeda, Y.; Oshio, H. *J. Phys. Chem. Solids* **1990**, *51*, 941.
(22) Schenker, S.; Hauser, A. *J. Am. Chem. Soc.* **1994**, *116*, 5497.
(23) Maeder, M.; Zuberbuehler, A. D. *Anal. Chem.* **1990**, *62*, 2220.

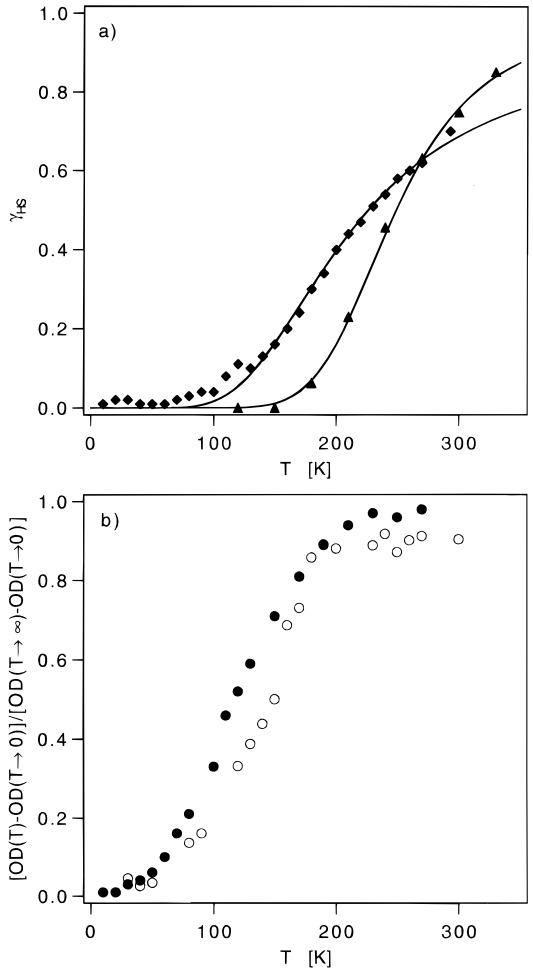

Figure 2. Temperature dependence of (a) the HS fraction γ_{HS} and the corresponding least-squares fit of $[Fe(acpa)_2]PF_6$, (◆) experimental and (—) calculated with $\Delta H^\circ_{HL} = 504$ cm^{-1} and $\Delta S^\circ_{HL} = 2.23$ cm^{-1}/K, and $[Fe(Sal_2tr)]PF_6$, (▲) experimental and (—) calculated with $\Delta H^\circ_{HL} = 1170$ cm^{-1} and $\Delta S^\circ_{HL} = 4.7$ cm^{-1}/K, in P/Bn and (b) $[OD_{\tilde{\nu}}(T) - OD_{\tilde{\nu}}(T\rightarrow 0)]/[OD_{\tilde{\nu}}(T\rightarrow\infty) - OD_{\tilde{\nu}}(T\rightarrow 0)]$ of $[Fe(Sal_2tr)]PF_6$ doped into $[In(Sal_2tr)]PF_6$ (●) and dispersed in KBr (○).

Figure 2a shows the transition curve obtained from the experimental spectra using the spectra of Figure 1b and the calculated transition curve using the values for ΔH°_{HL} and ΔS°_{HL} of 504(93) cm^{-1} and 2.23(41) cm^{-1}/K, respectively, which resulted from the least-squares fitting procedure. In the solid state the corresponding values are 587 cm^{-1} and 3.03 cm^{-1}/K.[21] The transition curve is gradual with $T_{1/2}$ of ≈ 225 K. This is slightly larger than the value of ≈ 188 K reported for $[Fe(acpa)_2]PF_6$ in the solid state.[20,21] Furthermore, the spin transition in solution is more gradual than in the solid state.

In analogy to the above, $[Fe(Sal_2tr)]PF_6$ in P/Bn has an absorption band at 16 100 cm^{-1} ($\epsilon^{20K}_{max} = 3500$ L/mol cm) characteristic for the LS species and one at 20 450 cm^{-1} ($\epsilon^{330\,K}_{max} = 5000$ L/mol cm) characteristic for the HS species. This is in agreement with the absorption spectra of the same compound in an acetone solution given in the literature,[3] showing a LS and a HS band at 16 130 cm^{-1} ($\epsilon^{241\,K}_{max} = 2885$ L/mol cm) and 20 410 cm^{-1} ($\epsilon^{318\,K}_{max} = 4000$ L/mol cm), respectively. At 20 K in P/Bn the HS band has completely disappeared, but even at 330 K the LS fraction is still nonnegligible. Using the equation

$$OD_{\tilde{\nu}}(T) - OD_{\tilde{\nu}}(T\rightarrow 0) = \alpha\gamma_{HS} = \alpha[1 + \exp\{(\Delta H^\circ_{HL} - T\Delta S^\circ_{HL})/k_B T\}]^{-1}$$

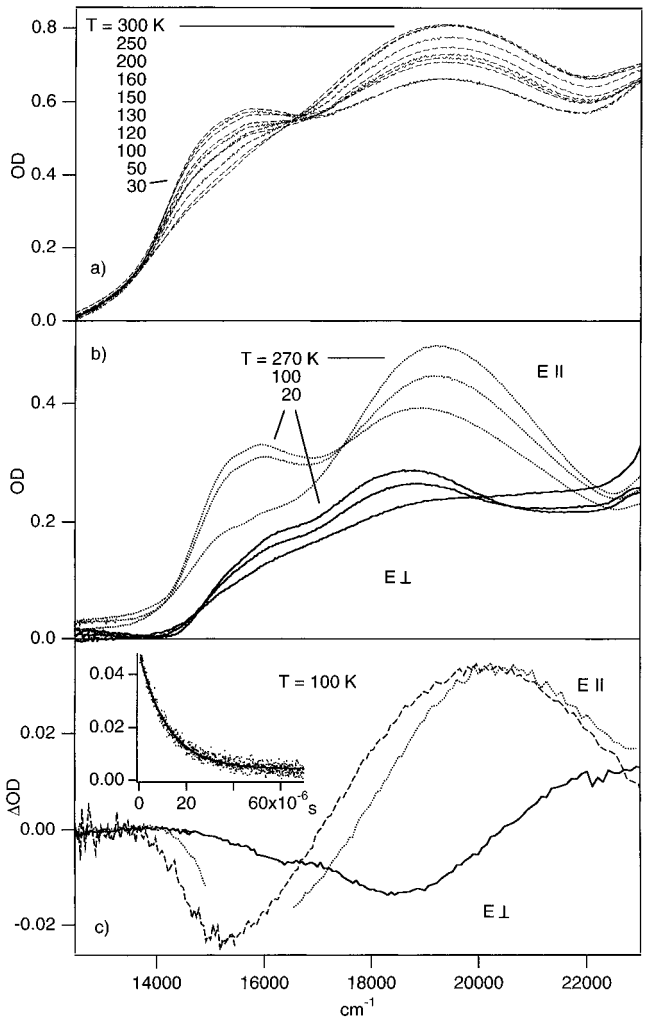

Figure 3. (a) Absorption spectra of $[Fe(Sal_2tr)]PF_6$ dispersed in KBr between 30 and 300 K. (b) Absorption spectra of $[In_{1-x}Fe_x(Sal_2tr)]PF_6$ ($x = 0.005$) between 20 and 250 K in $E_{||}$ (••) and $E_\perp$ (—) polarization. (c) Excited state difference absorption spectra at 100 K of $[Fe(Sal_2tr)]PF_6$ dispersed in KBr after pulsed laser excitation at 14 700 and 16 800 cm^{-1} (--) and doped into $[In(Sal_2tr)]PF_6$ after pulsed laser excitation at 15 625 and 17 240 cm^{-1} ($E_{||}$ (••) and $E_\perp$ (—)). Inset: HS → LS relaxation curve of $[In_{1-x}Fe_x(Sal_2tr)]PF_6$ at 100 K detected at 20 000 cm^{-1} after pulsed laser excitation at 15 625 cm^{-1}.

($\alpha = \Delta\epsilon_\lambda \cdot c \cdot d$), valid for $\gamma_{HS}(T\rightarrow 0) = 0$, and performing a three parameter least-squares fit, it is straight forward to extract a thermal transition curve from the experimental temperature dependence of the absorption spectra. Figure 2a shows the corresponding transition curve. The resulting thermodynamic parameters, $\Delta H^\circ_{HL} = 1170(118)$ cm^{-1} and $\Delta S^\circ_{HL} = 4.7(5)$ cm^{-1}/K, and $T_{1/2} = 250$ K are within the range observed for this complex in a series of solvents.[3]

Parts a and b of Figure 3 show the temperature dependent absorption spectra of $[Fe(Sal_2tr)]PF_6$ dispersed in KBr and doped into $[In(Sal_2tr)]PF_6$, respectively. Because of the dichroic behavior of the single crystals, the latter were recorded in mutually orthogonal polarisations, labeled $E_{||}$ and $E_\perp$ to the stronger absorption direction. The quantitative evaluation of the data is not as straightforward, because in contrast to solution data there is a substantial HS fraction even at the lowest temperatures, as is evident from the nonvanishing intensity of the HS band at 19 530 cm^{-1} in the 20 K spectra. A similar behavior has already been noted for neat $[Fe(Sal_2tr)]PF_6$,[19] and was attributed to the fact that in the crystal the Fe(III) complexes occupy two nonequivalent lattice sites, with only the complexes on one site showing a thermal spin transition. Instead of γ_{HS},

Figure 2b shows the function

$$[OD_{\tilde{\nu}}(T) - OD_{\tilde{\nu}}(T\rightarrow 0)]/[OD_{\tilde{\nu}}(T\rightarrow\infty) - OD_{\tilde{\nu}}(T\rightarrow 0)]$$

corresponding to the HS fraction of only those complexes which actually undergo the spin transition. There is no significant difference between $[Fe(Sal_2tr)]PF_6$ dispersed in KBr and $[In_{1-x}Fe_x(Sal_2tr)]PF_6$, $x = 0.005$, and with $T_{1/2} = 130$ and 120 K, respectively, both behave in much the same way as the neat compound.[19] Since the ionic radius of In(III) ($r = 80$ pm) is somewhat bigger than the one of Fe(III) in the HS state ($r = 65$ pm), a stabilization of the HS state is expected in the indium host, resulting in the slightly lower value for $T_{1/2}$. Using KBr as matrix, the question of a possible anion exchanche may arise. According to ref 19, $[Fe(Sal_2tr)]Br\cdot 2H_2O$ is a LS compound. As there is no indication of a temperature independent contribution to the LS intensity in the experimental spectra of Figure 3a, and as microcrystals on the order of several micrometers are clearly observable under a microscope, it may be concluded that $[Fe(Sal_2tr)]PF_6$ is only dispersed and not dissolved in KBr and that anion exchange is negligible.

All three transition curves of the $[Fe(Sal_2tr)]^+$ complex are gradual and have approximately equal slopes. As mentioned in the Introduction, cooperative effects do not seem to be important in this system.

3.2. Laser Flash Photolysis. Figure 1c shows the excited state difference absorption spectrum of $[Fe(acpa)_2]PF_6$ in P/Bn excited at 14 700 and 15 600 cm^{-1} and at a temperature of 100 K, where the system is predominately in the LS state. Excitation at two different wavelengths was necessary to obtain the entire spectrum, because of the interference of the background luminescence of the laser dye. There is a bleaching of the typical LS band, at the same time the absorption in the region of the HS band increases. This spectrum proves the light-induced state to be the HS state. In contrast to Fe(II) spin-crossover compounds, the quantum efficiency for the light-induced population of the HS state is on the order of a few percent only. In addition, it is temperature dependent, decreasing with decreasing temperature. Below 30 K the amplitude of the transient signal drops to below the detection limit. At 100 K the lifetime of the metastable HS state is ≈ 2 μs. The corresponding HS $\rightarrow$ LS relaxation curve, shown in the inset of Figure 1c, is slightly nonexponential due to the inhomogeneous environment provided by the amorphous matrix.

The excited state difference absorption spectra for $[Fe(Sal_2tr)]PF_6$ in KBr and for $[In_{1-x}Fe_x(Sal_2tr)]PF_6$ at 100 K are depicted in Figure 3c. The missing region of the $E_{\|}$ spectrum is due to the above-mentioned luminescence of the laser dye. As for the above compound, there is bleaching of the LS band and increased absorption in the region of the HS band. The single crystal data reflect the fact that the $E_{\perp}$ spectrum is dominated by LS bands only. At 100 K the lifetime of the light-induced HS state is ≈ 17 μs. The corresponding HS $\rightarrow$ LS relaxation curve, shown in the inset of Figure 3c, is single exponential, as is to be expected for this unimolecular process in the well-defined environment of a diluted single crystal.

The relaxation rate constants for the HS $\rightarrow$ LS relaxation for the two complexes $[Fe(Sal_2tr)]PF_6$ and $[Fe(acpa)_2]PF_6$ in the various matrices were determined as a function of temperature by monitoring the transient bleaching at the maximum of the respective LS bands (this is preferable to monitoring the transient absorption at the maximum of the HS band, because it is less prone to artifacts caused for instance by thermal lensing). In parts a and b of Figure 4, the observed relaxation rate constants k_{obs} for $[Fe(Sal_2tr)]PF_6$ dispersed in KBr and $[In_{1-x}Fe_x(Sal_2tr)]PF_6$ as well as for $[Fe(acpa)_2]PF_6$ dispersed in KBr and dissolved in P/Bn are plotted as $\ln[k_{obs}]$ vs $1/T$ (Arrhenius plot). For $T \ll T_{1/2}$, k_{obs} is equal to the HS $\rightarrow$ LS relaxation rate constant k_{HL}. In the region of the thermal spin transition the relation $k_{HL} = k_{obs}(1 - \gamma_{HS})$ holds. A common feature of all four curves is a classical Arrhenius type behavior above $\approx$100 K and a much less temperature dependent tunneling process below $\approx$80 K. The corresponding frequency factors A, activation energies E_a, transition temperature $T_{1/2}$ and low-temperature tunneling rate constants $k_{HL}(T\rightarrow 0)$, obtained for $[Fe(Sal_2tr)]PF_6$, $[Fe(acpa)_2]PF_6$ and $[Fe(bzpa)_2]PF_6$ dispersed in KBr and dissolved in P/Bn as well as for $[In_{1-x}Fe_x(Sal_2tr)]PF_6$, are collected in Table 1. Literature values for the activation parameters of $[Fe(Sal_2tr)]PF_6$ in a series of solvents are also included in Table 1.

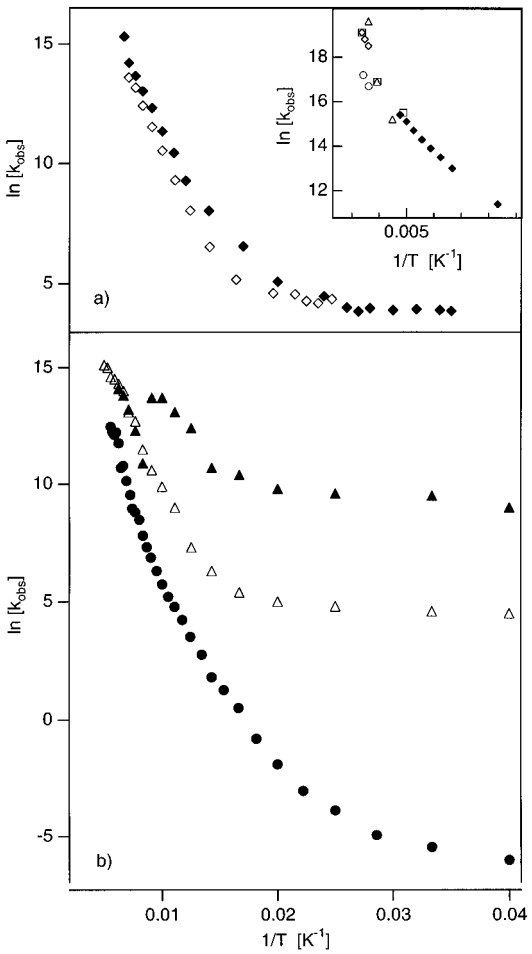

Figure 4. $\ln[k_{obs}(T)]$ vs $1/T$ for the HS $\rightarrow$ LS relaxation of (a) $[Fe(Sal_2tr)]PF_6$ dispersed in KBr (◇) and doped into $[In(Sal_2tr)]PF_6$ (◆), (b) $[Fe(acpa)_2]PF_6$ dispersed in KBr (△), in P/Bn (▲), and $[Mn_{1-x}Fe(II)_x(pic)_3]Cl_2\cdot MeOH$ (●).[8] Inset: Comparison of $\ln[k_{obs}(T)]$ vs $1/T$ for $[Fe(Sal_2tr)]PF_6$ in different solvents: in H_2O (◇),[5] in MeOH (○)[3] and (□),[5] in acetone (△)[5] and in P/Bn (◆).

$[Fe(Sal_2tr)]PF_6$ in KBr and doped into $[In(Sal_2tr)]PF_6$ behave quite similarly. The low-temperature tunneling rate constants $k_{HL}(T\rightarrow 0)$ are on the order of 100 s^{-1} and the activation energies are $\approx$740 cm^{-1}. This is a further indication that in this system cooperative effects are not important. In the inset of Figure 4a, the observed relaxation rate constants for $[Fe(Sal_2tr)]PF_6$ in P/Bn are compared to those reported in water,[4] methanol,[3,5] and acetone.[5] The dependence of the HS $\rightarrow$ LS relaxation on solvent, although not negligible, is rather small when considered in relation to the overwhelming temperature dependence. Furthermore, the results from different experimental methods, that is temperature jump,[3] ultrasonic relaxation,[4] and laser flash photolysis,[5] are in good agreement with each other.

Table 1. Activation Energy E_a, Frequency Factor A, Transition Temperature $T_{1/2}$, and Low-Temperature Tunneling Rate $k_{HL}(T\rightarrow 0)$ of $[Fe(Sal_2tr)]PF_6$, $[Fe(acpa)_2]PF_6$, and $[Fe(bzpa)_2]PF_6$ in Various Matrices

	E_a (cm^{-1})	A (s^{-1})	$T_{1/2}$ (K)	$k_{HL}(T\rightarrow 0)$ (s^{-1})
$[In_{1-x}Fe_x(Sal_2tr)]PF_6$	735	3.4×10^9	120	1.5×10^2
$[Fe(Sal_2tr)]PF_6$ in KBr	748	1.8×10^9	130	3.9×10^2
$[Fe(Sal_2tr)]PF_6$ in P/Bn	1254	4.2×10^{10}	250	10^2
$[Fe(Sal_2)tr]PF_6$ in H_2O[a]	1733	8.1×10^{11}	305	
$[Fe(Sal_2tr)]PF_6$ in MeOH[b]	1738	1.5×10^{11}	290	
$[Fe(Sal_2tr)]PF_6$ in MeOH[c]	1578	2.8×10^{11}	290	
$[Fe(Sal_2tr)]PF_6$ in acetone[c]	3301	5.3×10^{15}	280	
$[Fe(acpa)_2]PF_6$ in KBr	709	7.0×10^8	190	1.9×10^2
$[Fe(acpa)_2]PF_6$ in P/Bn			225	1.8×10^4
$[Fe(bzpa)_2]PF_6$ in KBr	880	2.6×10^8	220	3.3×10^2
$[Fe(bzpa)_2]PF_6$ in P/Bn	1280	4.4×10^8	240	5.1×10^4
$[Mn_{1-x}Fe_x(pic)_3]Cl_2 \cdot MeOH$[d]	1120	2×10^8	118	5.5×10^{-4}
$[Zn_{1-x}Fe_x(pic)_3]Cl_2 \cdot EtOH$[d]			95	2.5×10^{-3}

[a] Reference 4. [b] Reference 3. [c] Reference 5. [d] Reference 8.

For $[Fe(acpa)_2]PF_6$ dispersed in KBr, the low-temperature tunneling rate constant and the activation energy are not too different from the above. In the P/Bn solution, however, the low-temperature tunneling rate constant is 2 orders of magnitude larger, and there is an anomaly at the glass point, $T_g \approx 120$ K. The related compound $[Fe(bzpa)_2]PF_6$ shows a similar behavior. It looks as if the rigidity of the P/Bn glass matrix has the same effect on the HS $\rightarrow$ LS relaxation dynamics as an applied pressure. Below the glass point the measured relaxation rate constants are two orders of magnitude faster than in the KBr matrix. Above the glass point, in liquid P/Bn they behave more or less the same as in the KBr matrix. This point should not be given too much importance, however, as pulsed laser experiments performed on polymers and glasses at low temperatures are prone to artifacts due to bad heat dissipation.

For comparison with a typical Fe(II) spin-crossover compound, Figure 4b and Table 1 include the experimental data for the diluted mixed crystal $[Mn_{1-x}Fe_x(pic)_3]Cl_2 \cdot MeOH$ ($x = 0.0005$, pic = 2-picolylamine) taken from the literature.[8] As mentioned in the introduction, at elevated temperatures the relaxation rate constant for the Fe(II) system is only 1 order of magnitude smaller than for the Fe(III) systems. At low temperatures, it is about 6 orders of magnitude smaller.

4. Discussion

The thermal spin transition in Fe(III) compounds has been discussed before.[2,16,24,25] The transition curves are generally more difficult to determine experimentally than for Fe(II) compounds, because (a) Mössbauer spectra have to be evaluated using a dynamic model, and (b) for magnetic susceptibility data the usually unknown orbital contribution to the magnetic moment of the LS state has, in principle, to be considered. The values for ΔH°_{HL} and ΔS°_{HL} quoted in the literature have to be looked at with caution. The optical spectra shown here provide another method toward determining transition curves. Due to the strong overlap of the bands of LS and HS species and the temperature dependence of the individual band shapes (there are no truly isosbestic points), it is, unfortunately, not more accurate than the classical methods. Nevertheless, a combination of the three methods conveys a reasonable and consistent picture of the thermal spin transition in the title compounds. It is not the goal of this paper to dwell on this point. The temperature dependent spectra merely serve as a basis for the discussion of the HS $\rightleftharpoons$ LS relaxation. To begin with, the observation of a transient signal at a given wavelength following pulsed laser excitation only shows that a transient state is being populated, but it does not say anything about the nature of this state. It is only the comparison of the full excited state difference absorption spectrum with the temperature dependent spectra that allows an unambiguous assignment of the transient state to the HS state. The fact that in the dilute mixed crystal system $[In_{1-x}Fe_x(Sal_2tr)]PF_6$ the relaxation curves are single exponential within experimental accuracy shows that the HS $\rightarrow$ LS relaxation is a truly unimolecular process. Deviations from single exponential behavior in low-temperature glasses and KBr pellets are due either to local heating and temperature gradients or to inhomogeneities of the amorphous matrices rather than to the physics of the relaxation process as such.

As mentioned in the Introduction, the HS $\rightarrow$ LS relaxation may be treated quantum mechanically as a nonadiabatic multiphonon process.[6] Within the single configurational coordinate model the relaxation rate constant can be expressed as[26]

$$k_{HL}(T) = \frac{2\pi}{\hbar^2\omega} g_f \beta_{HL}^2 F_p(T) \qquad (1)$$

where $\hbar\omega$ is the vibrational frequency along the effective reaction coordinate, g_f the electronic degeneracy of the final state, β_{HL} the electronic matrix element given by higher order spin−orbit coupling and $F_p(T)$ the thermally averaged Franck−Condon factor. Assuming equal force constants for initial and final state

$$F_p(T) = \frac{\sum_m |\langle\chi_{m+p}|\chi_m\rangle|^2 e^{-m\hbar\omega/kT}}{\sum_m e^{-m\hbar\omega/kT}} \qquad (2)$$

The sum goes over all vibrational levels m of the initial state. In order to ensure energy conservation, the number of vibrational quanta n created in the final state is $m + p$, where $p = \Delta E^\circ_{HL}/\hbar\omega$ is the reduced energy gap. For the low-temperature tunneling rate constant

$$k_{HL}(T\rightarrow 0) = \frac{2\pi}{\hbar^2\omega} g_f \beta_{HL}^2 |\langle\chi_p|\chi_0\rangle|^2 = \frac{2\pi}{\hbar^2\omega} g_f \beta_{HL}^2 \frac{e^{-S}S^p}{p!} \qquad (3)$$

where the Huang-Rhys factor $S = {}^1/_2 f\Delta Q^2/\hbar\omega$ is the reorganization energy in units of vibrational quanta. A reasonable approximation to the reaction coordinate is the totally symmetric metal−ligand stretch vibration, as it is well-known from crystallographic data that it is mainly the metal−ligand bond length which is affected by the spin transition. With an average value of $\Delta r_{HL} \approx 0.12$ Å[15,16,25,27,28] ($\Delta Q = \sqrt{6}\Delta r_{HL}$), a typical vibrational frequency $\hbar\omega$ of 350 cm^{-1},[21] and a corresponding force constant f of 3×10^5 dyn/cm, a value for S of ≈25 may be estimated. The electronic matrix element β_{HL} calculated by second-order spin−orbit coupling via the low lying $^4T_2$ state is ≈ 40 cm^{-1}.[6]

In Table 2 the above values are compared to corresponding values typical for Fe(II) spin-crossover compounds.[8] Since for both Fe(II) and Fe(III) spin-crossover compounds the zero-point energy difference ΔE°_{HL} has to be on the order of the thermal energies, the reduced energy gaps for both are around unity. The key difference between Fe(II) and Fe(III) compounds is the horizontal displacement of the potential wells of the HS and the LS state relative to each other and thus the value of the

(24) Cambi, L.; Szegö, L.; Cassano, A. *Atti Acad. Naz. Lincei, Cl. Sci. Fis., Mat. Nat., Rend.* **1932**, *15*, 329.
(25) Maeda, Y.; Takashima, Y. *Comments Inorg. Chem.* **1988**, *7*, 41.
(26) Donnelly, C. J.; Imbush, G. F. *NATO ASI B Physics*; (DiBartolo, B., Ed.; Plenum Press: New York, 1991; Vol. 249, p 175.
(27) Milne, A. M.; Maslen, E. N. *Acta Crystallogr., B* **1988**, *44*, 254.
(28) Oshio, H.; Toriumi, K.; Maeda, Y.; Takashima, Y. *Inorg. Chem.* **1991**, *30*, 4252.

Table 2. Model Parameters of Typical $[Fe^{II}N_6]$ and $[Fe^{III}N_4O_2]$ Spin-Crossover Compounds

	Fe(II)[a]	Fe(III)		Fe(II)[a]	Fe(III)
β_{HL} (cm^{-1})	150	40[b]	f (dyn/cm)	2×10^5	3×10^5
Δr_{HL} (Å)	0.18	0.12[c]	S	45	25
$\hbar\omega$ (cm^{-1})	250	350[d]			

[a] Reference 8. [b] Reference 6. [c] References 25, 27, and 28. [d] Reference 21.

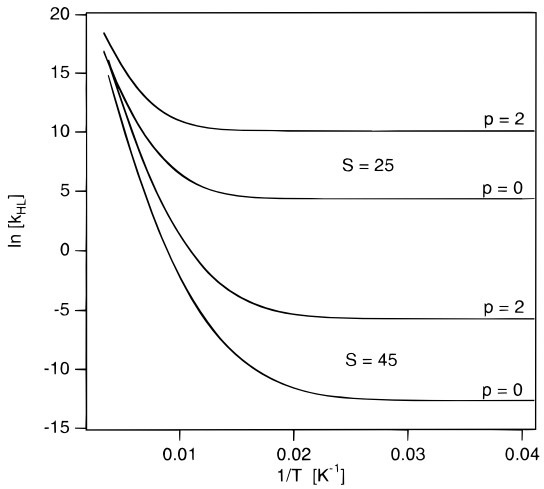

Figure 5. Calculated curves of $\ln[k_{HL}(T)]$ vs $1/T$ according to eq 1 using the model parameters in Table 2.

Huang−Rhys factor S. The smaller value of S translates into a smaller and narrower energy barrier between the two states and thus faster low-temperature tunneling for Fe(III) compounds as compared to Fe(II) compounds. In Figure 5, the HS → LS relaxation rate constants k_{HL} calculated according to eq 1 using the parameters of Table 2 for Fe(II) and Fe(III), respectively, are plotted as $\ln[k_{HL}]$ vs $1/T$. The reduced energy gap $p = 0$ may be regarded as a lower limit, and $p = 2$ represents a typical value for spin-crossover compounds. Clearly the general temperature behavior, that is a thermally activated process at elevated temperatures and tunneling at low temperatures, is as found experimentally. Furthermore, on the basis of the estimated values of S for Fe(II) and Fe(III), the at first sight amazing fact that at ambient temperature the relaxation rate constants differ only by 1 order of magnitude on average, whereas in the low-temperature tunneling region the HS → LS relaxation is several orders of magnitude faster for Fe(III) systems, is predicted theoretically.

In Figure 6 the low-temperature tunneling rate constants according to eq 3 are plotted as functions of the reduced energy gap p for both sets of parameters from Table 2. The values for S of 25 and 45 for Fe(III) and Fe(II), respectively, are to be regarded as average values. The experimental low-temperature tunneling rate constants are expected to lie within a comparatively narrow band of ±1 order of magnitude around the central line. Thus the estimated ratio of $k_{HL}(T\rightarrow 0)$ of Fe(III) and Fe(II) spin-crossover compounds with $p \approx 1$ is on the order of $10^{7\pm2}$. The experimental ratio of $k_{HL}(T\rightarrow 0)$ for the $[Mn_{1-x}Fe_x(pic)_3]Cl_2\cdot MeOH$ (5.5×10^{-4} s^{-1})[8] to $k_{HL}(T\rightarrow 0)$ for $[In_{1-x}Fe_x(Sal_2tr)]PF_6$ (1.5×10^2 s^{-1}), the two having approximately equal transition temperatures $T_{1/2}$ of 118 K and 120 K respectively and thus similar energy gaps, is 3.3×10^5, which is within this limit.

For Fe(II) compounds the expected exponential increase of $k_{HL}(T\rightarrow 0)$ with increasing value of p (inverse energy gap law) could be verified experimentally by taking $T_{1/2}$ as a measure for p.[9] The data for Fe(III) compounds presented here are not as straightforward to interpret. The data base is too small to show an overall trend relating $k_{HL}(T\rightarrow 0)$ to $T_{1/2}$. However, comparing the very similar systems $[Fe(acpa)_2]PF_6$ and $[Fe(bzpa)_2]PF_6$ both dispersed in KBr, $k_{HL}(T\rightarrow 0)$ increases with increasing $T_{1/2}$. The same holds for $[Fe(Sal_2tr)]^+$ in the solid state, that is for $[Fe(Sal_2tr)]PF_6$ in KBr, and in $[In(Sal_2tr)]PF_6$. Direct comparison of the two groups of systems is not possible, because the rather crude estimates and approximations of the single configurational coordinate do not take either the specific electronic structure, that is splittings due to low-symmetry ligand fields, or the individual vibrational structure into account. Also comparison of solid state data and solution data is not possible in this case. In particular, in $[Fe(acpa)_2]PF_6$ secondary effects, for instance specific solvent−solute interactions, seem to influence the HS → LS relaxation dynamics to a nonnegligible extent.

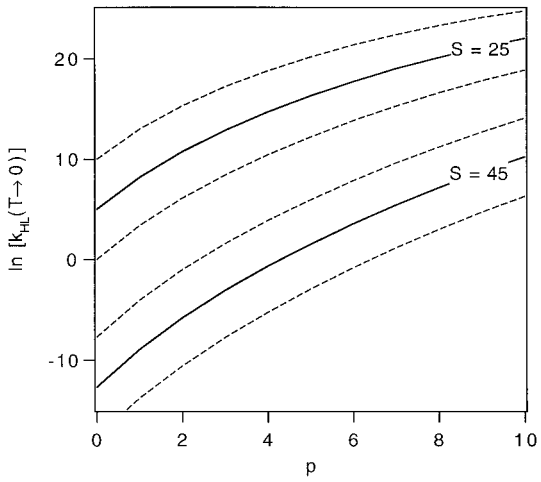

Figure 6. Calculated curves of the low-temperature tunneling rate constant, $\ln[k_{HL}(T\rightarrow 0)]$ in dependence of the reduced energy gap p according to eq 3 using the parameters in Table 2.

5. Conclusions

For both Fe(II) and Fe(III) spin-crossover compounds the HS → LS relaxation can be described as a nonadiabatic multiphonon process in the strong vibronic coupling limit, that is, with the Huang−Rhys factor S much larger than the reduced energy gap p. Within the series of Fe(II) compounds studied previously,[8,9] the chemical variation on the ligands provided a way to vary the zero-point energy difference ΔE°_{HL} and thus p between the HS and the LS state, while the bond length difference Δr°_{HL} was kept within a comparatively small range. This study allowed for a consistent estimate of an average value of 45 for the crucial Huang−Rhys parameter S as a measure for the horizontal displacement of the two potential wells relative to each other. With the extension to Fe(III) spin-crossover compounds Δr_{HL} and thus S have been varied too. Because of the $[FeN_4O_2]$ coordination for the Fe(III) compounds, as opposed to the $[FeN_6]$ coordination for the Fe(II) compounds, the single configurational coordinate model is a much cruder approximation for the former. Nevertheless, the value for S of 25, estimated from average bond length differences and reasonable assumptions regarding vibrational frequencies and force constants, explains the 7 orders of magnitude larger low-temperature tunneling rate constant for the HS → LS relaxation in Fe(III) compounds as compared to Fe(II) compounds at least semiquantitatively. At the same time the theory of nonadiabatic multiphonon relaxation predicts that the classical activation parameters for the high-temperature region are not too different for Fe(II) and Fe(III) spin-crossover compounds in agreement with a large body of experimental findings.

This study shows that, in order to understand the HS → LS relaxation dynamics at a quantum mechanically correct level, it is essential to perform experiments over a large temperature interval and preferably down to cryogenic temperatures.

A large number of photochemical and photophysical applications of transition metal compounds depend on a high quantum efficiency of an initial ISC process, as for instance the $^4T_2 \rightarrow {}^2E$ ISC of Cr^{3+} in the ruby laser,[29] or the $^1MLCT \rightarrow {}^3MLCT$ ISC process in photovoltaic cells based on $[Ru(bipy)_3]^{2+}$.[30,31] A thorough and quantitative understanding of ISC dynamics and of the parameters which govern them is thus important on its own right. Spin-crossover compounds are model systems for studying ISC dynamics, because these parameters can be determined independently. In contrast, for most other compounds, where thermally nonaccessible states participate, the relevant parameters have to be determined indirectly from spectroscopic data. More often than not these do not carry enough information to determine excited state distortion unambiguously, despite the undoubted progress that has been made in that respect.[32,33] Furthermore, spin-crossover compounds are currently being treated as possible candidates for thermo-optical data processing.[34]

Acknowledgment. We thank H. U. Güdel (Universität Bern, Switzerland) for the use of the equipment and M. Maeder (University of Newcastle, Australia) for his advice with the least-squares global fits. We also thank the "Schweizerische Nationalfonds", the "Hochschulstiftung der Universität Bern", and the "Stiftung der Portlandcementfabrik" for financial support.

IC960010U

(29) Imbush, G. F.; Yen, W. M. In *Lasers, Spectroscopy and New Ideas*; W. M., Yen, M. D., Levenson, Eds.; Optical Sciences; Springer-Verlag: Berlin, Heidelberg, Germany 1987; Vol. 54, p 248.
(30) Juris, A.; Balzani, V.; Barigelletti, F.; Campagna, S.; Belser, P.; von Zelewski, A. *Coord. Chem. Rev.* **1988**, *84*, 85.
(31) Grätzel, M. *Comments Inorg. Chem.* **1991**, *12*, 93.
(32) (a) Wilson, R. B.; Solomon, E. I. *J. Am. Chem. Soc*. **1980**, *102*, 4085. (b) Wilson, R. B.; Solomon, E. I. *Inorg. Chem*. **1978**, *17*, 1729.
(33) Zink, J. I.; Kim Shui. K. S. In Advances in Photochemistry; Volmann, D. M., Hammond, G. S., Neckers, D. C., Eds.; John Wiley: New York, 1991; Vol. 16, p 119.
(34) Jay. Ch.; Groliere, R.; Kahn, O.; Kröber, J. *Mol. Cryst. Liq. Cryst. Sci. Technol., Sect. A* **1993**, *234*, 255.